High second-order optical nonlinearities in thermally poled sol-gel silica

V. Pruneri, G. Bonfrate, and P.G. Kazansky

Optoelectronics Research Centre, Southampton University, Southampton SO17 1BJ, UK

Fax: ++44-1703-593149, Tel: ++44-1703-593083, Email: vp3@orc.soton.ac.uk

H. Takebe and K. Morinaga

Department of Materials Science and Technology, Graduate School of Engineering Sciences, Kyushu University, Kasuga, Fukuoka 816, Japan

M. Kohno and K. Kuwasaki

R & D Laboratories, Nippon Steel Chemical Co. Ltd., Kitakyushu, Fukuoka 804, Japan

T. Takeuchi

R & D Division, Seiko Epson Corp., Suwa, Nagano 392, Japan

Abstract

Silica glass samples prepared by a sol-gel process, the mixture of silica sol for gelation and colloidal silica particles, have been thermally poled in vacuum by continuous high voltage (8-12 kV) at elevated temperature (280 ^{0}C). High second-order nonlinearities (>1pm/V), located under the anodic surface, have been measured and the values are higher than those obtained in fused silica glass, poled under the same conditions. A model for thermal poling is suggested which explains the experimental results in sol-gel silica and the difference between thermal poling of sol-gel and fused silica. The granular structure and the boundaries of sol-gel silica seem to play a major role in establishing the electrical properties of the depletion layer during and after poling.

In 1991 it was shown that permanent and large second-order nonlinearities could be produced in fused silica using thermal poling [1]. This has promoted considerable exciting investigations on alternative poling techniques: corona poling [2], electron beam implantation [3]; on device aspects: linear electro-optic modulation [4] and quasi-phase-matched fibers [5]; on material aspects: sol-gel silica glass [6], tellurite glass [7], silicate [8], phosphate glasses [9], and soda-lime [10]; and on poling conditions [6,7,11]. In thermally poled fused silica the second-order nonlinearity is located in a thin (tens of microns) region below the anodic surface of the glass sample and can be explained by a very high frozen-in electric field (close to the breakdown field) in the depletion region which induces a second-order nonlinear susceptibility ($\chi^{(2)}$) either via third-order suceptibility or orientation of dipoles which possess second-order hyperpolarizability. Although the latter mechanism is not ruled out yet, there are strong indications that the former gives the right picture for thermal poling in fused silica. An important feature of thermal poling is that it produces nonlinear layers which are more stable than those obtained by other poling techniques, e.g. UV-assisted poling [12].

Since a feature of glass materials consists in the diversity of chemical composition (for example different impurities such as Na^+ and OH [1,6] and defect centers such as oxygen deficient centers [13] may affect the value of $\chi^{(2)}$ in poled silica glasses), many researchers expect to develop novel second-order nonlinear glasses with higher $\chi^{(2)}$ compared to that in fused silica glass. Silica glasses prepared via sol-gel methods are very promising materials since they are synthesized at low

temperatures (800 to 1800 °C), and they can potentially lead to simple and economic routes for fabricating optical elements.

Recently poling of the whole thickness (about 1 mm) of sol-gel silica glass was reported [6]. This result excites particular interest because it may give an evidence of dipole alignment in the glass (the field in the volume of 1 mm thick sample is too small to induce the measured $\chi^{(2)}$ via third-order monlinearity). In this work we have carried out measurements of $\chi^{(2)}$ and its distribution in sol-gel samples, thermally poled using high voltages 8-12 kV. The results indicate surface $\chi_{33}^{(2)}$ greater than 1 pm/V over 15-20 μm (and not over the whole 2 mm thickness). These $\chi^{(2)}$ values are higher than those in fused silica, subjected to the same poling conditions and, as previously reported [14], to even higher voltages (up to 20 kV) and temperatures (440 °C). We believe that the superior performance of poled sol-gel silica over poled fused silica is due to the capability of storing higher electric-fields in the depletion region, as a consequence of higher breakdown threshold.

Silica glass samples were prepared by modified sol-gel process [15] using mixture of the sol for gelation and colloidal silica particles to avoid cracking and bloating during densification. Sol-gel silica samples were finally melted at temperature ranging from 1600 °C and 1800 °C for 10 minutes in an Ar atmosphere or in vacuum (see table 1). A commercial fused-silica glass (Herasil 1) was used for comparison. A Si anode and a stainless steel cathode were pressed onto both sides of the samples which were subsequently poled at 280 °C in a vacuum chamber at ~10^{-8}atm with poling voltages and

times listed in table 1. The poling time given in this paper is the sum of the actual time at 280 ^{0}C and of the cooling time (~2 minutes) to reach temperatures of ~220 ^{0}C (the contribution to poling below this temperature can be considered not significant). The fundamental source used in the SH experiments was a mode-locked and Q-switched Nd:YAG laser which delivers ~1 W average power at 1.064 μm.

To characterize the nonlinear layer we performed Makers fringes measurements by tilting the poled sample, so that the SH power could be measured as a function of the angle of incidence [1]. As example of Makers fringes, figure 1 shows those obtained for sol-gel 4 for the two different poling conditions of table 1. In table 1 are listed the maximum values of SH power obtained by optimizing the angle of incidence. The sol-gel samples show much higher SH signals than fused silica samples poled in similar conditions. In fact the poling time for fused silica was shorter than that for sol-gel silica in order to limit the nonlinear thickness (which increases with poling time and voltage) to values comparable with those in sol-gel, so that a better comparison for the $\chi^{(2)}$ of the nonlinear layer could be carried out. Assuming a uniform nonlinear layer (square-like distribution under the anodic surface) one can infer the thickness of the nonlinear layer from the Makers measurements and the value of $\chi^{(2)}$ can be calculated by comparing with crystalline quartz [1,6]. The values of the nonlinear thickness (which were also assessed by etching techniques) and the $\chi_{33}^{(2)}$ (calculated assuming $\chi_{33}^{(2)} = 3\ \chi_{31}^{(2)}$) are listed in table 1 apart from sol-gel samples 1 and 3, as the SH signal was not uniform along the poled area for these samples (see fig. 2) making unreliable the Makers

fringes measurement. The tilting varies the amount of poled area invested by the beam which contributes to the SH signal, making necessary a good uniformity to avoid variations which would make impossible a correct interpretation of the Makers fringes results.

Fig. 2 shows the SH signal when the sample is moved perpendicularly to the plane of incidence (along the poled area) for sol-gel samples 1 and 4 (the behaviour of sol-gel 3 is similar to sol-gel 1 whereas sol-gel 2 and herasil are similar to sol-gel 4). The pump beam has a spot size ($1/e^2$ intensity-radius) at the beam waist of ~ 50 μm. In the sol-gel samples 1 and 3, which gave non-uniform SH signal, we observed two-lob structure of the brightest SH spots. The SH signals in these two lobs were observed to be π out of phase. Magnified image of the near-field patterns revealed pair-crescent moon structure of SH spots (inset of fig.2). Moreover we also observed, by moving the sample relative to the pump, that the fringe-like distribution of SH signal is following certain curved lines, revealing some granular structure in the sample. The granular structure was also present in a much weaker form in sol-gel samples 2 and 4, which also show a considerably weaker inohomogeity of SH signal, whereas it was absent in the poled fused silica samples (Herasil 1).

Recent results, including those reported in this paper, cannot be explained in the framework of a single charged carrier model. In particular the time dependence of thermal poling and the values of the nonlinear thicknesses obtained indicate that the process takes place in two stages: the rapid formation, within tens of seconds, of negatively charged region depleted with cations (Na^+) followed by a slower process which is responsible for charge separation within the depletion region [11,16].

The time scale of this process depends on the charged species involved, on the poling atmosphere (air or vacuum) and on the poling conditions, such as temperature and applied voltage. It has been proposed [16] that during thermal poling in air H^- or H_3O^+ are driven by the high electric field at the anode into the region depleted by Na^+, thus neutralizing the negative charges left behind by Na^+. At the same time, the region depleted with Na^+ increases and this ion exchange process results in the forward movement of the negative depleted region. For increasing time, the nonlinear thickness increases, thus leading to a decrease of the electric field, hence of $\chi^{(2)}$. The poling stops when the electric field near the anode drops to values corresponding to which H^+/H_3O^+ ions cannot be driven into the sample and when the total voltage drops across the depletion region, so that the movement of Na^+ in the bulk stops.

We believe that, because of the high field, negative species such as electrons [17,18] and oxygen ions [19] are likely to move and contribute to the second stage. The movement of these negative carriers keep the electric field to levels below the breakdown field and can be seen as an equivalent process to the injection of H^+/H_3O^+. Right after the Na^+ depleted region is formed, the electric field peaks at the anode surface causing currents of electrons or oxygen ions. Because of this, the peak of the electric-field moves further from the anode surface with increasing time, leading to an increase in the nonlinear thickness. Correspondingly the electric field and the $\chi^{(2)}$ become smaller, while the resistivity in the depletion layer increases. The poling stops when the increase in resistivity and voltage in the depletion region makes negligeble the Na^+ drift in the bulk of the sample.The

described electric-field driven motion of negative charges is the dominat mechanism during thermal poling in vacuum since the injection of H^+/H_3O^+ is limited, whereas in air atmosphere the latter is probably more significant. Indeed we have made measurements, to be reported in a different publication, that point out the importance of the poling atmosphere (air or vacuum) and support this model.

In the view of this model we explain our experimental results as follows. The structure of sol-gel glasses can be seen as made by SiO_2 grains with boundaries containing most of the OH and SiOH groups. Therefore, in sol-gel silica samples there may be channels along the traces of grain boundaries which help to move or trap charge carriers. The importance of the boundaries for thermal poling is supported by the observed two-lob SH patterns (inset fig.2) which may be explained by the space charge field, concentrated at these boundaries. The electric field has opposite directions from both sides of the space charge and produces two sposts of antiphase SH signals. The dark region in the middle of the two-lob structure corresponds to the location of charge. The observed stronger inhomogenity in sol-gel 1 compared to sol-gel 2 (which have similar granular structure) is probably related to the higher OH concentration in the former sample creating more defects (charge carriers or traps) at the boundaries. Sol-gel 3 is similar in structure and has comparable OH content to sol-gel 1 although melted in vacuum rather than Ar atmosphere, thus giving similar SH behaviour. Sol-gel 4 is melted at higher temperature than sol-gel 3, resulting in a smaller granular structure and higher evanescent electric field inside the grains, thus leading to more uniform poling and greater SH performances.

Contrary to sol-gel samples the structure of herasil 1 is very uniform and there is no evidence of any grains or channels. In Herasil 1 the main carrier responsible for the depletion layer formation (first stage of poling) is Na^+ whose concentration is ~ 1ppm because the other cations, such as H^+, have much lower mobility. In sol-gel, instead, because of the channels containing OH and SiOH groups and the lower content of Na^+ (~0.23 ppm), it is likely that H^+ also moves during the first poling stage contributing to the formation of the depletion layer. Regarding the second poling stage (charge separation in the depletion region) in herasil 1 the evolution of the depletion layer is expected to be different because of the absence of the channels at the boundaries which influence the conductivity properties. Bearing in mind that in our model the electric-field which can be stored in the depletion layer is closely related to the electrical conductivity of negative charges such as electrons and oxygen ions, the fact that fused silica produce thicker nonlinear layers and lower $\chi^{(2)}$ than those of sol-gel silica is a strong indication of higher conductivity and lower breakdown field in the depletion region. This is also supported by the fact that in fused silica the nonlinear layer growth (whose speed is proportional to the conductivity) is much faster than in sol-gel, i.e. shorter poling times give thicker nonlinearities. The reason for a lower conductivity and higher breakdown field in sol-gel silica is related to the fact that the grain boundaries act as trapping centres for the negative carriers.

In conclusion, we have shown that high second-order nonlinearities can be induced by thermal poling in silica prepared by sol-gel method. These nonlinearities develop under the anodic surface and are higher than those obtained in fused silica, poled in similar conditions. The experimental results are interpreted on the basis of a model which considers the movement of electrons and

oxygen ions and explains the differences between sol-gel and fused silica in terms of different conductivity and breakdown field in the depletion region. The granular structure and the electrical properties at the grain boundaries seem to play a major role in the poling process.

V. Pruneri acknowldges Pirelli Cavi for his fellowship. G. Bonfrate acknowledges DERA Malvern for his studentship.

References

1. R.A. Myers, N. Mukherjee, and S.R.J. Brueck, Optics Lett. **16**, 1732 (1991).
2. A. Okada, K. Ishii, K. Mito, and K. Sasaki, Appl.Phys.Lett. **60**, 2853 (1992).
3. P.G. Kazansky, A. Kamal, and P.St.J. Russell, Optics Lett. **18**, 693 (1993).
4. A.C. Liu, M.J.F. Digonnet, and G.S. Kino, Optics Lett. **19**, 466 (1994).
5. V. Pruneri, G. Bonfrate, P.G. Kazansky, C. Simonneau, P. Vidakovic, and J.A. Levenson, Applied Phys. Lett. **72**, 1007 (1998).
6. H. Nasu, H. Okamoto, K. Kurachi, J. Matsuoka, K. Kamiya, A. Mito, and H. Hosono, J.Opt.Soc.Am.B **12**, 644 (1995).
7. K.Tanaka, K.Kashima, K.Hirao, N.Soga, A.Mito and H.Nasu, Jpn.J.Appl.Phys. **32**, L843 (1993).
8. O. Sugihara, M. Nakanishi, H. Fujimura, C. Egani, N. Okamoto, J.Opt.Soc.Am.B **15**, 421 (1998) .
9. Y. Watanabe, N. Takeshita, T. Tsuchiya, H. Hosono, and H. Kawazoe, OSA 1995 Technical Digest Series **22**, 92 (1995).
10. F.C. Garcia, I.C.S. Carvalho, E. Hering, W. Margulis, and B. Lesche, Appl. Phys. Lett. **72**, 3252 (1998).
11. H. Takebe, P.G. Kazansky, P.St.J. Russell, and K. Morinaga, Optics Lett. **20**, 468 (1996).
12. T. Fujiwara, M. Takahashi, and A.J. Ikushima, Electronics Lett. **33**, 980 (1997).
13. L.J. Henry, Optics Lett. **20**, 1592 (1995).
14. A.C. Liu, D. Pureur, M.J. Digonnet, G.S. Kino, and E.J. Knystautas, OSA 1997 Technical

Digest Series **17**, 302 (1997).

15. M. Toki, S. Miyashita, T. Takeuchi, S. Kanabe, and A. Kochi, J. Non-Crystalline Solids **100**, 479 (1988).

16. T.G. Alley, R.A. Myers, and S.R.J. Brueck, OSA 1997 Technical Digest Series **17**, 293 (1997).

17. P.G. Kazansky, and P.St.J. Russell, Optics Comm. **110**, 611 (1994).

18. U.K. Krieger and W.A. Lanford, J. Non-Cryst. Solids **102**, 50 (1988).

19. D.E. Carlson, J. Am. Ceram. Soc. **57**, 291 (1974).

Table 1 Poling of sol-gel silica and fused silica (Herasil 1) in vacuum at 10^{-8} atm and 280 °C: OH concentration, melting conditions (temperature and atmosphere), poling conditions, maximum SH signal, nonlinear thickness and $\chi_{33}^{(2)}$ for the nonlinear layer. The nonlinear coefficient d_{33} is ~ $\chi_{33}^{(2)}/2$. For sol-gel 1 and 3 the SH signal was transversely non uniform, making impossible a reliable measurement of the thickness and $\chi^{(2)}$.

Silica	**Poling**	**SH signal (a.u.)**	**Thickness (μm)**	$\chi_{33}^{(2)}$ **(pm/V)**
Sol-gel 1 OH~150ppm 1800 °C, Argon	8 kV, 7', 280 °C	4 (non uniform)	–	–
Sol-gel 2 OH<1ppm 1800 °C, Argon	8 kV, 7', 280 °C	1	18	0.29
Sol-gel 3 OH~100ppm 1600 °C, vacuum	8 kV, 7', 280 °C	3 (non uniform)	–	–
Sol-gel 4 OH~100ppm 1800 °C, vacuum	8 kV, 10', 280 °C 12 kV, 7', 280 °C	7 15	15 20	0.73 1.07
Herasil 1 OH~150ppm 2100 °C, oxyhydrogen flame	8 kV, 4', 280 °C 12 kV, 2', 280 °C	1 0.4	24 36	0.3 0.41

Figure captions

1. Makers fringes for sol-gel 4 for the two different poling conditions listed in table 1. The dashed and continuous curves are the calculated lines for a uniform (square-shape) nonlinear layer of 20 and 15 μm thickness respectively.

2. Distribution of SH signals along the poled area (obtained by moving the sample perpendicularly to the beam and the plane of incidence) in poled sol-gel silica samples 1 and 4. The inset is a near field pattern of SH signal in poled sol-gel sample 1 where two two-lob structures (in each pair the lobs are π phase shifted with respect to each other) at the grain boundaries are evident.

V. Pruneri et al., '*High second-order optical...*', **fig.1**

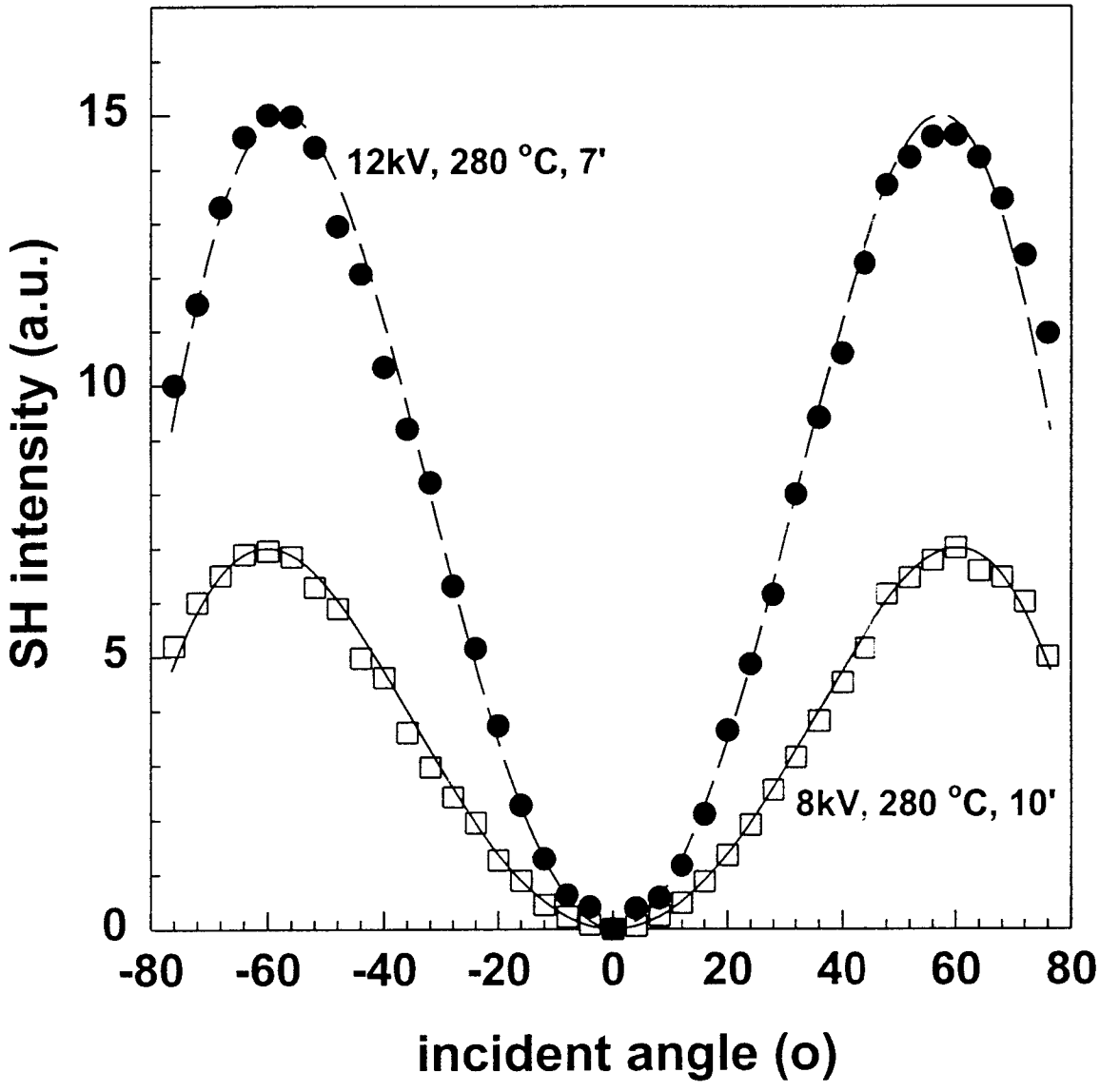

V. Pruneri et al., '*High second-order optical...*', **fig.2**